

(Li, Na, K)OH hydration bonding thermodynamics : solution self-heating

Sun, Chang Qing; Yao, Chuang; Chen, Jiasheng; Liu, Xinjuan; Zhang, Xi; Huang, Yongli

2018

Sun, C. Q., Chen, J., Yao, C., Liu, X., Zhang, X., & Huang, Y. (2018). (Li, Na, K)OH hydration bonding thermodynamics : solution self-heating. Chemical Physics Letters, 696, 139-143. doi:10.1016/j.cplett.2018.02.038

<https://hdl.handle.net/10356/85920>

<https://doi.org/10.1016/j.cplett.2018.02.038>

© 2018 Elsevier. All rights reserved. This paper was published in Chemical Physics Letters and is made available with permission of Elsevier.

Downloaded on 09 Apr 2024 16:55:20 SGT

(Li, Na, K)OH Hydration Bonding Thermodynamics: Solution Self-Heating

Chang Q Sun^{1,*}, Jiasheng Chen², Chuang Yao¹, Xinjuan Liu³, Xi Zhang⁴, Yongli Huang^{2,*}

Abstract

The resultant energy of solvent H-O bond exothermic elongation by $O:\rightleftharpoons O$ repulsion, featured at $<3100\text{ cm}^{-1}$, and the solute H-O bond endothermic contraction by bond-order-deficiency, at 3610 cm^{-1} , heats up the (Li, Na, K)OH solutions. The solution temperature increases linearly with the number fraction of the ordinary O:H-O bonds transiting into their hydration states. The elongated H-O bond emits $>150\%$ the O:H cohesive energy of 0.095 eV that caps the energy dissipating by molecular motion, thermal fluctuation, diffusion, and even evaporation. Therefore, the intramolecular H-O bond relaxation dictates the OH^- solvation bonding thermodynamics and the performance of basic solutions.

Keywords: Solvation; hydrogen bond; thermodynamics; Raman spectroscopy

¹ Chongqing Key Laboratory of Extraordinary Bond Engineering and Advanced Materials Technology (EBEAM), Yangtze Normal University, Chongqing 4081410, China (20161042@yznu.cn); NOVITAS, Nanyang Technological University, Singapore 639798 (ecqsun@ntu.edu.sg)

² School of Materials Science and Engineering, Xiangtan University, Xiangtan 411105 (1403277520@qq.com; huangyongli@xtu.edu.cn)

³ Institute for Coordination Bond Engineering, China Jiliang University, Hangzhou 310018, China (14A0502088@cjl.edu.cn)

⁴ Institute of Nanosurface Science and Engineering, Shenzhen University, Shenzhen 518060, China; (Zh0005xi@szu.edu.cn)

1. Introduction

Exothermic and endothermic reactions are of great importance to both basic and engineering sciences [1-3], as well as efficiency of drug functioning[4]. However, why the OH^- hydration heats up its solution remains to be resolved. A comprehensive discussion [5] on the thermodynamic chemistry occurred in liquids, solids, and semiconductor materials suggested that the concurrent understandings are mainly within the framework of classical thermodynamics in terms of enthalpy [6, 7] and Gibbs energy [8]. The heat generation at reaction is mainly attributed to the solute-solvent electron transportation[5, 9] and molecular interactions[10], water molecular motion dynamics [11], H-O correlation [12]. Inter- and intra-molecular cooperative interactions govern the path, ultimate outcome, and efficiency of aqueous solvation [13].

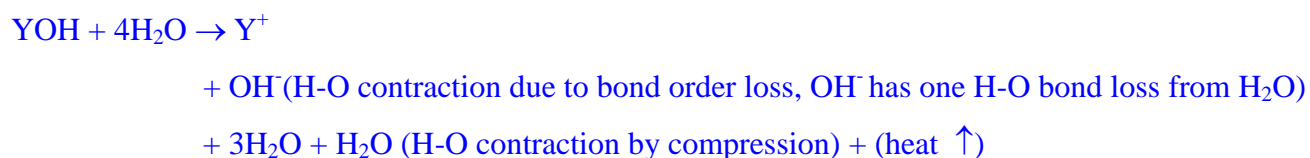
The pump-probe ultrafast infrared absorption spectroscopy investigation [14] suggests that the spectral signal for the OH^- solvation decays its intensity in 200 fs and this process is followed by a thermalization that becomes slower with increasing the solute concentration. The molecular thermalization proceeded by water molecular rotation, reorientation, and diffusion is suggested to be responsible for the solvation thermodynamics [15]. Two processes of molecular motion relaxations occur upon NaOH hydration in bulk water [16] and in water clusters [17]. One is the slow process on 200 ± 50 fs time scales and the other faster dynamics on 1–2 ps scales. Density functional theory calculations suggest that the OH^- hydration shall contains $\text{OH}^- \cdot 3\text{H}_2\text{O}$ molecules [3] and the hydrating molecular structure undergoes evolution by reorientation at heating [18]. However, quantitative information and atomistic insight into the solvation intramolecular bonding and intermolecular nonbonding thermodynamics and their cooperativity still open for examination.

Extending our recent findings on the YOH ($\text{Y} = \text{Li}, \text{Na}, \text{K}$) solvation Raman spectroscopy [19], we show herewith quantitatively that the energy difference between the solvent H-O bond elongation by $\text{O}:\rightleftharpoons:\text{O}$ compression and the solute H-O bond contraction due to HO^- bond-order deficiency heats up the YOH solutions. The solution temperature $T(\text{C})$ varies linearly with the fraction number $\Delta f(\text{C})$ of the H-O bonds transiting from the mode of ordinary water to the elongated and contracted states upon the YOH being hydrated.

2. Principles

2.1. YOH Solvation Phonon Spectrometrics

The YOH solvation proceeds as follows [19] with involvement of possible bonding thermodynamics, as listed in Table 1:



Solvation in water dissolves the YOH into a Y^+ ion and an OH^- hydroxide. The Y^+ leaves one of its electron behind the OH^- that keeps its sp^3 -orbital hybridization with three lone pairs “:” on it. This process adds three “:” and one H^+ into the solvent consisting N value of H_2O molecules and turns the initial 2N protons into 2N + 1 and the “:” from 2N to 2N+3. The excessive two “:” forms uniquely the $\text{O}:\rightleftharpoons:\text{O}$ repulsive nonbond, called super-HB, for convenience, as Figure 1a inset illustrated. The stronger $\text{O}:\rightleftharpoons:\text{O}$ repulsion compresses its neighboring $\text{O}:\text{H}-\text{O}$ bond. Mechanical compression shortens the $\text{O}:\text{H}$ and lengthens the $\text{H}-\text{O}$ cooperatively [20], see Figure 1b inset. On the other hand, the OH^- solute is subject to bond order-deficiency, which shortens its due $\text{H}-\text{O}$ bond [21].

Table 1. Bonding thermodynamics of YOH solvation.

Energy absorption Q_a	Solvent H-O bond thermal contraction by temperature raising	significant
	solute H-O contraction by bond-order-deficiency [22]	significant
	hydrating H-O bond contraction by Y^+ polarization [23]	Negligible because YX solvation and polarization change little the solution temperatures
Energy emission Q_e	YOH dissolution into Y^+ and OH^- [19]	
	solvent H-O elongation by $\text{O}:\rightleftharpoons:\text{O}$ repulsion [19]	significant

	O:H elongation by Y^+ polarization [23]	Negligible due to tiny O:H energy
Energy dissipation	molecular motion and structure fluctuation	With little contribution to energy absorption or emission
Q_{dis}	heat loss due to the non-isothermal calorimetric detection	Cause error tolerance

Figure 1a and b display the full-frequency Raman spectra for YOH solutions [19], which agrees with those probed with infrared spectra from YOH and YOD solutions [17, 24, 25]. Solvation broadens and flattens the H-O vibration peak towards lower frequencies. The peak position corresponds to the bond stiffness $(\omega_x)^2 \propto (E/d^2)_x$ of the x segment of the O:H-O bond ($x = L$ and H for the O:H and the H-O, respectively). The E_x is the bond energy and d_x the bond length. The O:H-O bond consists the weaker O:H (~ 0.1 eV, ~ 200 cm^{-1}) intermolecular van der Waals bond (vdW) and the stronger H-O (~ 4.0 eV; 3200 cm^{-1}) intramolecular covalent bond, which are coupled by the Coulomb repulsion between electron lone pairs on adjacent oxygen ions [22]. At 4°C temperature, $d_L = 1.70$ and $d_H = 1.0$ Å. If a specific bond becomes shorter and it turns to be stiffer, a blue shift of its vibration peak occurs, and vice versa. One can thus judge how the bond length and energy change from the phonon band frequency shift and how the O:H and the H-O segment cooperate. The rest bond bending vibration modes are out of immediate concern.

It has been extensively affirmed that the O:H-O bond disparity and the O-O repulsivity dictate the extraordinary adaptivity, sensitivity, recoverability of water and ice subjecting to stimulation [22]. As Figure 1b inset illustrated, the segmented O:H-O bond relaxes oppositely. Compression shortens the softer O:H nonbond and lengthens the H-O bond cooperatively. The O:H relaxes always more than the stiffer H-O bond does with respect to the H^+ coordination origin under stimulation. On the other hand, bond-order-deficiency shortens the intramolecular covalent bond spontaneously for the undercoordinated systems [21].

Figure 1c and d display the differential phonon spectra (DPS) for the O:H and the H-O phonons. The DPS is the difference between the spectra collected from water with and without solvation upon both spectral peak area normalized. Minimizing the artefact such as the cross-section of mode reflectivity,

the DPS resolves the fraction (peak area) and stiffness (frequency shift) of the O:H-O bonds transiting from the mode of ordinary water to the hydration. Compared with the inset DPS for water under compression, the O: \rightleftharpoons :O has the same but much stronger effect of compression on the phonon relaxation at the critical pressure, 1.33 GPa, for the room-temperature water-ice transition [26].

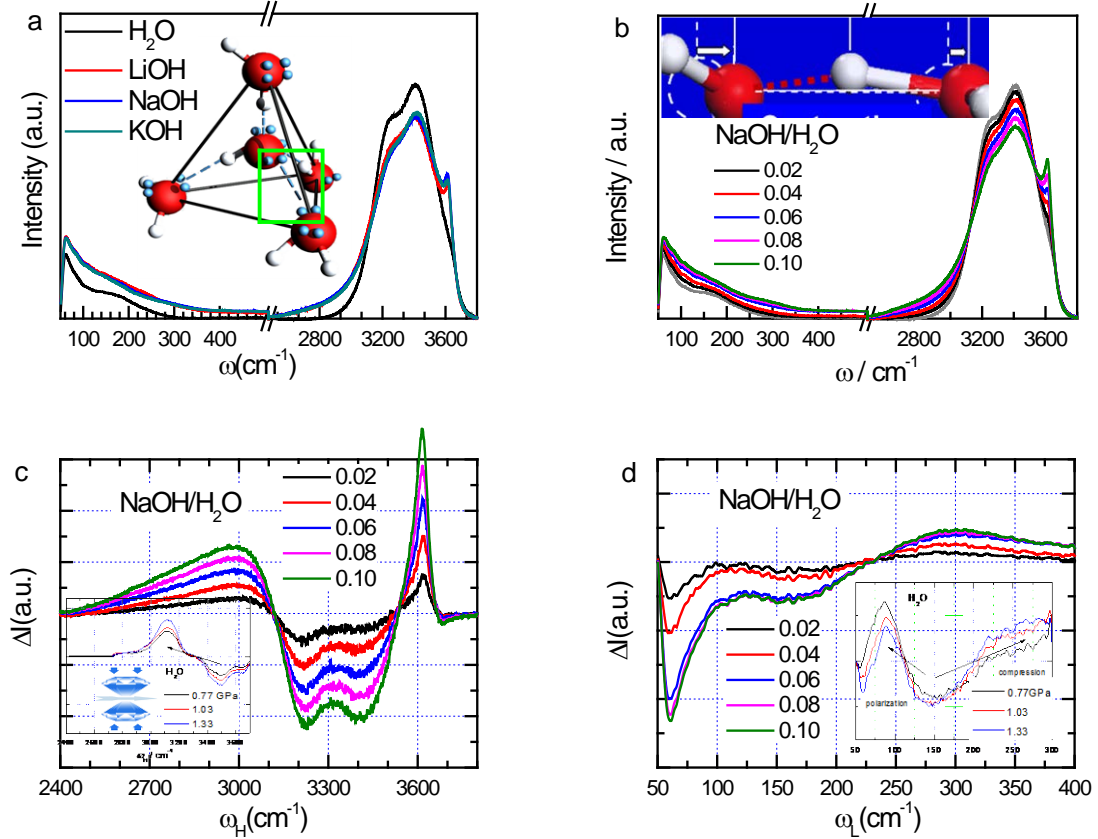


Figure 1. Full-frequency Raman spectroscopy for (a) YOH/H₂O of the same concentration and (b) concentrated NaOH/H₂O solutions and (c, d) the DPS profiles [19]. Inset **a** illustrates the central HO⁻ replacement of the 2H₂O unit cell, which derives an O: \rightleftharpoons :O bond as framed. Inset **b** shows the O:H-O bond cooperative relaxation under O: \rightleftharpoons :O compression, which has the same effect of pressure on the O:H-O bonds DPS as insets c and d demonstrated [19]. The O:H-O bond compression proceeds by O:H contraction and H-O elongation [22].

The solvent H-O bond elongation by O: \rightleftharpoons :O compression and the solute H-O contraction by bond-order-deficiency resolve two spectral features in the DPS shown in Figure 1c and d. The broader H-O

peak at $< 3100\text{ cm}^{-1}$ suggests long spatial decay of the $\text{O}:\leftrightarrow\text{O}$ compression; the sharp H-O peak at 3610 cm^{-1} features the localized nature of the solute H-O bond. The two DPS peaks may clarify that the longer $200 \pm 50\text{ fs}$ lifetime of the 3610 cm^{-1} H-O phonon features the slower OH^- motion dynamics and the other shorter lifetime on $1\text{--}2\text{ ps}$ scales is related to the lower-frequency $<3100\text{ cm}^{-1}$ elongated solvent H-O bond vibration upon HO^- solvation[19] in NaOH solutions[16, 17]. Integrating the DPS spectral peaks results in the $f(\text{C})$ that features the fractions of the H-O bonds transiting from the ordinary water to the elongated ($<3100\text{ cm}^{-1}$) and shortened (3610 cm^{-1}) states of hydration.

2.2. YOH Hydration Bonding Thermodynamics

According to Pauling [27], energy stores only in the chemical bonds and the energy emission or absorption proceeds by bond relaxation. Bond dissociation and elongation emit energy, but bond formation and contraction absorb energy, leading to the respective exothermic and endothermic reaction. However, energy dissipation by molecular motion and structure fluctuation contribute insignificantly to the change of solution temperature. Table 1 suggested thermodynamics involved in YOH solvation under the non-adiabatic calorimetric detection, and the significance of the bonding thermodynamic process.

3. Results and Discussion

3.1. Solution Temperature versus the Fraction of Bond Transition

To seek for the correspondence between the solution temperature $T(\text{C})$ and the $f(\text{C})$ for YOH solutions, we detected *in-situ* the solution temperature using a regular thermometer in a glass beaker under the ambient of $25\text{ }^\circ\text{C}$. The solution was stirred using a magnetic bar rotating in the beaker in 5 Hz frequency. Figure 2 plots the solute concentration-resolved $T(\text{C})$ and the $f(\text{C})$ for the fraction of H-O bonds transiting into $<3100\text{ cm}^{-1}$ and 3610 cm^{-1} upon solvation.

Excitingly, the $T(\text{C})$ correlates linearly to the $f(\text{C})$ profiles, irrespective of the solutes. Figure 2d compares the time needed to heat the solutions to the highest possible temperatures. KOH is more easily dissolved than the rest two. This thermal transportation relaxation time in second or minute time scales is completely different from the lifetime in the time-resolved infrared spectroscopy. The infrared

measures the molecular motion dynamics by monitoring the spectral signal decay of the H-O bond at a certain frequency at the fs ~ ps level [14-17, 28-31]. The infrared spectral lifetime changes with the solution viscosity, molecular drift diffusivity and the incident beam frequency, etc., with hopeful information on the intramolecular bonding dynamics.

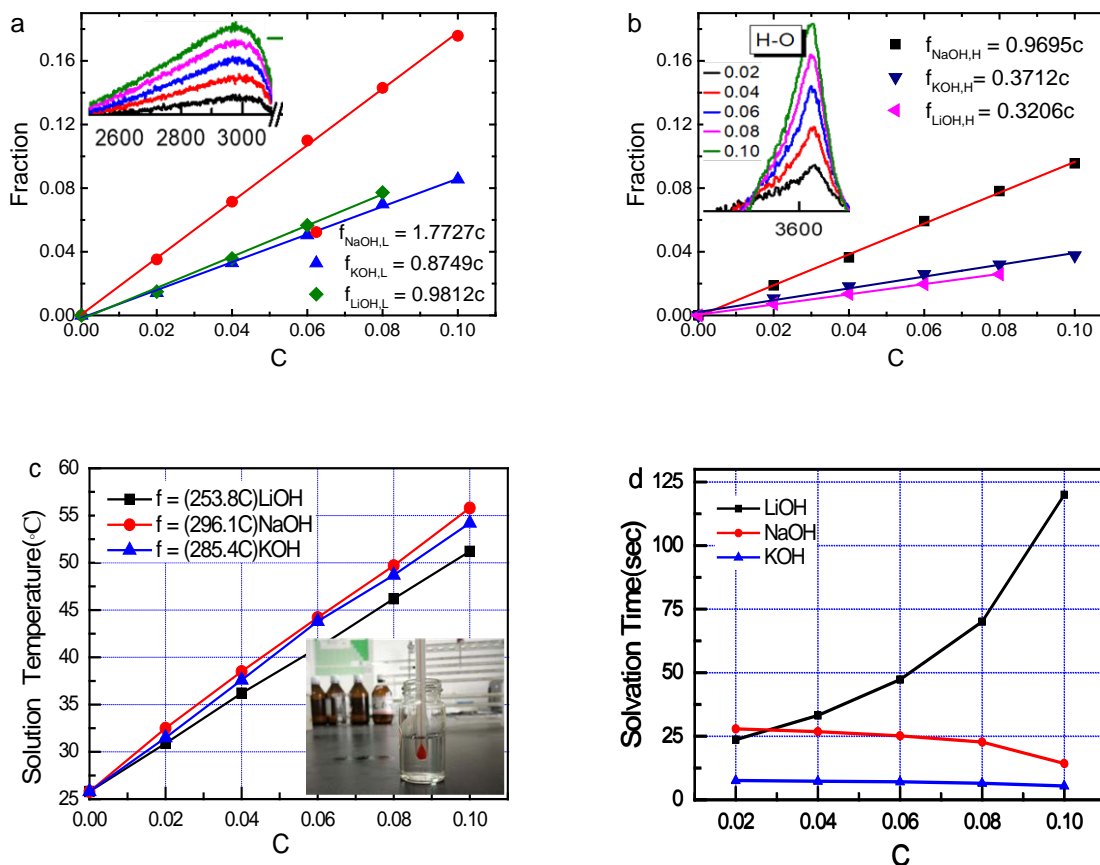


Figure 2. Concentration dependence of the fraction coefficients for (a) <3100 cm⁻¹ and (b) 3610 cm⁻¹ peaks of the (Li, Na, K)OH solutions, (c) the solution temperatures (inset a shows calorimetric detection set up), and (d) the thermal relaxation time required to reach the highest possible solution temperature.

3.2. Energetic Quantification

One could be able to estimate the energy exchange during solvation by considering the significant bonding thermodynamics given in Table 1:

$$\sum_3 Q_{e,i}(C) - \sum_3 Q_{a,j}(C) - \sum_2 Q_{dis,l}(C) = 0$$

$$\sum_3 Q_{e,i}(C) - \sum_3 Q_{a,j}(C) - \sum_2 Q_{dis,l}(C) = 0$$

Only three processes are significant. The energy Q_0 heating up a unit mass solution ($m = 1$ unit) from T_i to T_f by increasing the solute concentration up to C_M equals ($h_0 = 4.18 \text{ J}(\text{g}\cdot\text{K})^{-1} = 0.00039 \text{ eV}(\text{bond}\cdot\text{K})^{-1}$ is the specific heat for liquid water):

$$\int_0^{Q_0} dq = h_0 \int_0^1 dm \int_0^{C_M} \frac{dt(C)}{dC} dC = h_0 T(C_M)$$

$$\int_0^{Q_0} dq = h_0 \int_0^1 dm \int_0^{C_M} \frac{dt(C)}{dC} dC = h_0 T(C_M)$$

(1)

The energy difference ΔQ between the exothermic solvent H-O elongation and the endothermic solute H-O contraction heats up the solution. Only the $f_e(C)$ and $f_a(C)$ numbers of the hydrating bonds contribute to heat exchange. One can thus obtain the ΔQ ,

$$\int_0^{Q_e} dq_e - \int_0^{Q_a} dq_a = \left[h_e \int_0^{f_e} dm_e - h_a \int_0^{f_a} dm_a \right] \int_{T_i}^{T_f} dt = [h_e f_e - h_a f_a] T(C_M)$$

$$\int_0^{Q_e} dq_e - \int_0^{Q_a} dq_a = \left[h_e \int_0^{f_e} dm_e - h_a \int_0^{f_a} dm_a \right] \int_{T_i}^{T_f} dt = [h_e f_e - h_a f_a] T(C_M)$$

(2)

One may approximate that the energy emission per bond h_a is compatible to the energy absorption h_e for estimation, thus,

$$Q_e = h_e T(C_M) = \frac{h_0 T(C_M)}{f_e - f_a h_a / h_e} \approx \frac{h_0 T(C_M)}{f_e - f_a}, (\text{with } h_e \approx h_a)$$

$$Q_e = h_e T(C_M) = \frac{h_0 T(C_M)}{f_e - f_a h_a / h_e} \approx \frac{h_0 T(C_M)}{f_e - f_a}, (\text{with } h_e \approx h_a)$$

(3)

Table 2 tabulates the outcome showing that the H-O elongation by $\text{O}:\rightleftharpoons:\text{O}$ compression emits at least 150% the O:H cohesive energy (E_L) of 0.095 eV at room temperature [22]. It is thus justified that the energy remnant of the solvent H-O exothermic elongation and the solute H-O endothermic contraction heats up the solution.

Table 2. Derivative of energy emission from the H-O bond elongation by O: \rightleftharpoons :O compression.

YOH	C _M	f _e /C	f _a /C	T _M /C	h _e /h ₀	Q _e (eV/bond)	Q _e /E _L
LiOH	0.08	0.981	0.321	253.8	1.515	0.150	1.58
NaOH	0.1	1.773	0.970	296.1	1.245	0.144	1.52
KOH	0.1	0.875	0.371	285.4	1.984	0.221	2.33

One can also estimate the energy emission from the elongated H-O bond from the DPS (<3100 cm⁻¹) profile with the documented values of (d_H , E_H , ω_H) = (1.0 Å, 4.0 eV, 3200 cm⁻¹) for bulk water [22], and for basic solvent (1.10~1.05 Å, E_2 , 2500~3000 cm⁻¹). Differentiating the nature logarithm of the expression, $\omega^2 \propto E/d^2$, yields,

$$\Delta E = 2E \left(\frac{\Delta d}{d} + \frac{\Delta \omega}{\omega} \right) = 2 \times 4.0 \times \left(\frac{0.10 \sim 0.05}{1} + \frac{(2500 \sim 3000) - 3200}{3200} \right) = \begin{cases} -0.95 & (2500 \text{ cm}^{-1}) \\ -0.10 & (3000 \text{ cm}^{-1}) \end{cases}$$

$$\Delta E = 2E \left(\frac{\Delta d}{d} + \frac{\Delta \omega}{\omega} \right) = 2 \times 4.0 \times \left(\frac{0.1 \sim 0.05}{1} + \frac{(2500 \sim 3000) - 3200}{3200} \right) = \begin{cases} -0.95 & (2500 \text{ cm}^{-1}) \\ -0.10 & (3000 \text{ cm}^{-1}) \end{cases} \quad (4)$$

Indeed, the H-O bond elongation losses its cohesive energy from 4.0 by 0.10~0.95 eV depending on its frequency shift. Therefore, the exothermic H-O bond elongation by O: \rightleftharpoons :O compression is certainly the intrinsic and primary source for heating up the YOH solutions.

4. Conclusions

A combination of the DPS and calorimetric detection has clarified that intramolecular H-O bond relaxation serves as sources heating up the (Li, Na, K)OH solutions. The energy emission per H-O bond is at least 150% of the O:H cohesive energy at 0.095 eV that caps the energy dissipating by molecular motion, thermal fluctuation, diffusion, and even evaporation. The intramolecular H-O bond relaxation induced by molecular O: \rightleftharpoons :O repulsion and the bond-order-deficiency governs the solvation bonding

thermodynamics and the performance of the YOH aqueous solutions. Observations demonstrate not only the essentiality of extending the convention of solvation molecular dynamics to hydration bonding thermodynamics but also the power of the DPS in resolving the number and energetics of hydrogen bond transition from ordinary water to hydration.

Acknowledgment

Financial support received from the Natural Science Foundation (No. 11502223) and Science Challenge Project (No. TZ2016001) of China, Zhejiang Province (No. LY18E060005), Hunan Province (No. 2016JJ3119), and Shen Zhen (No. 827000131).

References

1. M.R. Rahimpour, M.R. Dehnavi, F. Allahgholipour, D. Iranshahi, and S.M. Jokar, *Assessment and comparison of different catalytic coupling exothermic and endothermic reactions: A review*. Applied Energy, **99**: 496-512, (2012).
2. R.C. Ramaswamy, P.A. Ramachandran, and M.P. Duduković, *Coupling exothermic and endothermic reactions in adiabatic reactors*. Chemical Engineering Science, **63**(6): 1654-1667, (2008).
3. W.H. Robertson, E.G. Diken, E.A. Price, J.-W. Shin, and M.A. Johnson, *Spectroscopic determination of the OH⁻ solvation shell in the OH⁻-(H₂O) *n* clusters*. Science, **299**(5611): 1367-1372, (2003).
4. N. Shahrin, *Solubility and Dissolution of Drug Product: A Review*. International Journal of Pharmaceutical & Life Sciences, **2**(1), (2013).
5. J.B. Rosenholm, *Critical evaluation of dipolar, acid-base and charge interactions I. Electron displacement within and between molecules, liquids and semiconductors*. Advances in Colloid and Interface Science.
6. Konicek J and W. I., *Thermochemical properties of some carboxylic acids, amines and N-substituted amides in aqueous solution* Acta Chem. Scand, **25**(5): 1461-1551, (1971).
7. E.L. Ratkova, D.S. Palmer, and M.V. Fedorov, *Solvation Thermodynamics of Organic Molecules by the Molecular Integral Equation Theory: Approaching Chemical Accuracy*. Chemical Reviews, **115**(13): 6312-6356, (2015).
8. G. Graziano, *Hydration thermodynamics of aliphatic alcohols*. PCCP, **1**(15): 3567-3576, (1999).
9. A.M. Ricks, A.D. Brathwaite, and M.A. Duncan, *IR Spectroscopy of Gas Phase V(CO₂)*n*+ Clusters: Solvation-Induced Electron Transfer and Activation of CO₂*. Journal of Physical Chemistry A, **117**(45): 11490-8, (2013).

10. Zaichikov A and K.y. M., *Structural and thermodynamic properties and intermolecular interactions in aqueous and acetonitrile solutions of aprotic amides*. Journal of Structural Chemistry, **54**(2): 336–344, (2013).
11. M. Wohlgemuth, M. Miyazaki, M. Weiler, M. Sakai, O. Dopfer, M. Fujii, and R. Mitrić, *Solvation dynamics of a single water molecule probed by infrared spectra--theory meets experiment*. Angewandte Chemie International Edition, **53**(52): 14601-4, (2014).
12. C. Velezvega, D.J. McKay, T. Kurtzman, V. Aravamuthan, R.A. Pearlstein, and J.S. Duca, *Estimation of Solvation Entropy and Enthalpy via Analysis of Water Oxygen-Hydrogen Correlations*. Journal of Chemical Theory & Computation, **11**(11): 5090, (2015).
13. K. Haldrup, W. Gawelda, R. Abela, R. Alonso-Mori, U. Bergmann, A. Bordage, M. Cammarata, S.E. Canton, A.O. Dohn, and T.B. Van Driel, *Observing solvation dynamics with simultaneous femtosecond X-ray emission spectroscopy and X-ray scattering*. The Journal of Physical Chemistry B, **120**(6): 1158-1168, (2016).
14. L. Liu, J. Hunger, and H.J. Bakker, *Energy relaxation dynamics of the hydration complex of hydroxide*. The Journal of Physical Chemistry A, **115**(51): 14593-14598, (2011).
15. J. Hunger, L. Liu, K.-J. Tielrooij, M. Bonn, and H. Bakker, *Vibrational and orientational dynamics of water in aqueous hydroxide solutions*. The Journal of Chemical Physics, **135**(12): 124517, (2011).
16. M. Thämer, L. De Marco, K. Ramasesha, A. Mandal, and A. Tokmakoff, *Ultrafast 2D IR spectroscopy of the excess proton in liquid water*. Science, **350**(6256): 78-82, (2015).
17. A. Mandal, K. Ramasesha, L. De Marco, and A. Tokmakoff, *Collective vibrations of water-solvated hydroxide ions investigated with broadband 2DIR spectroscopy*. J Chem Phys, **140**(20): 204508, (2014).
18. R.-J. Lin, Q.C. Nguyen, Y.-S. Ong, K. Takahashi, and J.-L. Kuo, *Temperature dependent structural variations of OH⁻(H₂O)_n, n= 4–7: effects on vibrational and photoelectron spectra*. Physical Chemistry Chemical Physics, **17**(29): 19162-19172, (2015).
19. Y. Zhou, D. Wu, Y. Gong, Z. Ma, Y. Huang, X. Zhang, and C.Q. Sun, *Base-hydration-resolved hydrogen-bond networking dynamics: Quantum point compression*. Journal of Molecular Liquids, **223**: 1277-1283, (2016).
20. C.Q. Sun, X. Zhang, and W.T. Zheng, *Hidden force opposing ice compression*. Chem Sci, **3**: 1455-1460, (2012).
21. C.Q. Sun, X. Zhang, J. Zhou, Y. Huang, Y. Zhou, and W. Zheng, *Density, Elasticity, and Stability Anomalies of Water Molecules with Fewer than Four Neighbors*. J. Phys. Chem. Lett., **4**: 2565-2570, (2013).
22. Y.L. Huang, X. Zhang, Z.S. Ma, Y.C. Zhou, W.T. Zheng, J. Zhou, and C.Q. Sun, *Hydrogen-bond relaxation dynamics: Resolving mysteries of water ice*. Coordination Chemistry Reviews, **285**: 109-165, (2015).
23. Y. Zhou, Y. Huang, Z. Ma, Y. Gong, X. Zhang, Y. Sun, and C.Q. Sun, *Water molecular structure-order in the NaX hydration shells (X= F, Cl, Br, I)*. Journal of Molecular Liquids, **221**: 788-797, (2016).
24. Y. Crespo and A. Hassanali, *Characterizing the local solvation environment of OH⁻ in water clusters with AIMD*. The Journal of chemical physics, **144**(7): 074304, (2016).

25. S.T. Roberts, P.B. Petersen, K. Ramasesha, A. Tokmakoff, I.S. Ufimtsev, and T.J. Martinez, *Observation of a Zundel-like transition state during proton transfer in aqueous hydroxide solutions*. Proceedings of the National Academy of Sciences, **106**(36): 15154-15159, (2009).
26. Q. Zeng, T. Yan, K. Wang, Y. Gong, Y. Zhou, Y. Huang, C.Q. Sun, and B. Zou, *Compression icing of room-temperature NaX solutions (X= F, Cl, Br, I)*. Physical Chemistry Chemical Physics, **18**(20): 14046-14054, (2016).
27. L. Pauling, *The Nature of the Chemical Bond*. 3 ed. 1960, Ithaca, NY: Cornell University press.
28. T. Brinzer, E.J. Berquist, Z. Ren, S. Dutta, C.A. Johnson, C.S. Krisher, D.S. Lambrecht, and S. Garrett-Roe, *Ultrafast vibrational spectroscopy (2D-IR) of CO₂ in ionic liquids: Carbon capture from carbon dioxide's point of view*. The Journal of chemical physics, **142**(21): 212425, (2015).
29. Z. Ren, A.S. Ivanova, D. Couchot-Vore, and S. Garrett-Roe, *Ultrafast structure and dynamics in ionic liquids: 2D-IR spectroscopy probes the molecular origin of viscosity*. The journal of physical chemistry letters, **5**(9): 1541-1546, (2014).
30. Q. Zhang, T. Wu, C. Chen, S. Mukamel, and W. Zhuang, *Molecular mechanism of water reorientational slowing down in concentrated ionic solutions*. Proceedings of the National Academy of Sciences: 201707453, (2017).
31. S.T. van der Post, C.S. Hsieh, M. Okuno, Y. Nagata, H.J. Bakker, M. Bonn, and J. Hunger, *Strong frequency dependence of vibrational relaxation in bulk and surface water reveals sub-picosecond structural heterogeneity*. Nat Commun, **6**: 8384, (2015).

